Cylindrical Transmitting Coil for Two-Dimensional Omnidirectional Wireless Power Transfer

Nam Ha-Van ⓘ , *Member, IEEE*, Yining Liu ⓘ, Prasad Jayathurathnage ⓘ , *Member, IEEE*, Constantin R. Simovski ⓘ, and Sergei A. Tretyakov ⓘ , *Fellow, IEEE*

***Abstract*—Megahertz-range wireless power transfer has become a promising approach for increasing spatial freedom of charging. This article proposes a cylindrical-shaped coil, which can produce the homogeneous magnetic field in a plane. The coil consists of two helical windings, which are wound to guide the current in opposite directions. A single power source is used to excite the transmitter without any current amplitude or phase control circuits. Furthermore, since the parasitic capacitance of the coil is not negligible due to the complexity of the coil shape, we develop a general equivalent model with parasitic capacitance for the analysis of complex coils. The system efficiency of the proposed omnidirectional wireless power transfer device is validated by a practical experiment. The measured dc-to-dc efficiency of approximately 72.4% and the load power of 13 W are demonstrated for the proposed wireless charging system at 6.78-MHz operating frequency. Finally, we verify that the electromagnetic exposure satisfies the safety regulations.**

***Index Terms*—Cylindrical transmitting coil, omnidirectional, specific absorption rate (SAR), wireless power transfer (WPT).**

I. INTRODUCTION

WIRELESS power transfer (WPT) has become rather ubiquitous because of its advantages in applications such as consumer electronic products, portable devices, robotics, electric vehicles, and biomedical implants [1]–[6]. In the modern trend of this research domain, omnidirectional WPT has been investigated with the goal to overcome the restrictions of conventional directional WPT systems [7]–[10]. Indeed, most wireless charging systems have the limitation of charging direction, which requires the receiver coils to be placed in a specific position or within a restricted receiving region. Therefore, when the receiving coil is shifted out from the desired position, the

performance of the WPT system is dramatically reduced in aspects of the output power and efficiency [11]–[13].

Different methods are studied to enhance the performance of WPT systems in expanding the positional freedom of wireless charging. In [14], an omnidirectional WPT system with three orthogonal transmitting (Tx) coils connected in series that has orientation-insensitive characteristics with three orthogonal receiving (Rx) coils was proposed. However, the complexity of the Rx structure is unsuitable and incompatible with compact single-Rx devices. Most omnidirectional WPT systems use several power sources to feed orthogonal Tx coils with some phase and current control systems [9], [15]–[17]. For instance, the basic mathematical theory of a two-dimensional (2-D) omnidirectional WPT system was proposed using two orthogonal coils with nonidentical current control to determine the Rx device's orientation and transfer the power toward the load [18]. In [19], a technique with load detection and power flow control is used to deliver the power to the targeted loads. However, these techniques need external measuring and a feedback control loop using oscilloscopes and controller units, which are prohibitively expensive in practice. To simplify the control method, a single-source modified Tx coil structure was implemented in [20], which can expand the magnetic field surrounding the Tx coil in 2-D space. However, the generated magnetic field of this cubic Tx coil is not perfectly 2-D omnidirectional due to wire coupling at the edges of the cubic structure. Likewise, an approximately omnidirectional dual-band WPT based on four-coil topology using a source loop was proposed in [21]. The source loop is designed to have two parallel coils that drive the current in the same direction, leading to very weak coupling. Moreover, an asymmetrically positioned vertical connector was used in both the source loop and repeater, creating a shadow zone.

It is clear that the state-of-the-art proposals for omnidirectional WPT systems can be categorized into two types: 1) Multiple Tx coils are connected with multiple power sources and the phases and amplitudes of coil currents are dynamically controlled depending on the receiver positions; and 2) single Tx structure connected with a single power source, but it has some blind spots with very small electromagnetic coupling. Therefore, having a simple solution for fully omnidirectional WPT without need for any active control is still an unsolved challenge. This article proposes a novel Tx structure that enables fully 2-D omnidirectional power transfer only using a single power source. The main objective of this work is to introduce a new coil structure that can yield a truly 2-D omnidirectional
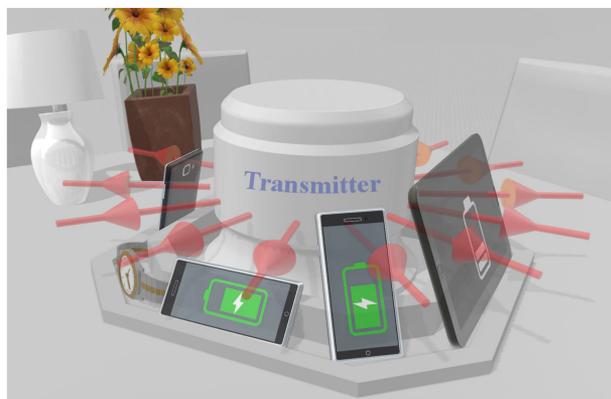
Fig. 1.　Considered scenario of omnidirectional wireless power transfer in consumer applications.

WPT without any blind spots, not requiring any active control or tuning. This enables Rx devices to be charged equivalently at any angular positions around the Tx antenna. In addition, compared to conventional omnidirectional WPT systems with multiple Tx coils connected to multiple power sources, we propose a single Tx coil fed by a single power source without any active control of amplitude or phase, which will greatly reduce the complexity and cost.

A conceptual illustration of the proposed omnidirectional wireless charging system for mobile and portable device applications is shown in the concept illustration of Fig. 1. The Tx charger can be set on a table, generating magnetic field to couple to all surrounding Rx devices placed in grooves or stand rings with a diversity of possible orientations. The red arrows show the magnetic field distribution in the horizontal plane, where the receiver devices are positioned. In other words, a new cylindrical Tx coil structure is proposed to transfer power in 2-D omnidirectional space such that receivers can be placed or moved freely without compromising power delivery. To achieve this goal, we configure magnetic field in an unusual manner by guiding the current flows in two opposite directions of two parallel helical coils. We construct and comprehensively study a model of the proposed coil. We adopt a single power source Tx structure, which does not need any current amplitude or phase control mechanism. Therefore, the use of the proposed topology significantly reduces the complexity and cost of the device.

In order to primarily justify the 2-D omnidirectional characteristic of the proposed coil, the mutual inductance, a crucial factor of the WPT system, is studied in comparison between the calculations and experiment. Furthermore, we consider the parasitic capacitance of the coil in an equivalent circuit model because of its inevitable effect at 6.78-MHz operating frequency. Experimental investigations of the fabricated prototype certify the WPT performance. Finally, electromagnetic field safety, which is one of the key limitations in the use of WPT systems, is assessed by studies of the specific absorption rate (SAR) value to guarantee human safety and complying with relevant regulations.

This article is organized as follows. The analysis of the WPT system with the proposed Tx coil is presented in Section II.

Here, the magnetic field of the Tx coil is evaluated as well as the mutual inductance between the Tx and Rx coils. The circuit model and system analysis are also presented in this section. Next, in Section III, we present fabricated and measured cylindrical Tx and Rx coils in a complete WPT system with a class EF_2 inverter and a rectifier to fully validate the proposed WPT system performance. Finally, a context of a consumer application with the SAR validation is described in Section IV, followed by conclusions.

II. Analysis of the Proposed 2-D Omnidirectional WPT

In general, WPT systems have a drawback of anisotropic power transfer, because the generated magnetic field of the coil is not homogeneous. The main reason is that even a set of three identical orthogonal coils produces field whose amplitude varies with the observation angle. Therefore, the coupling coefficient varies with changing of the receiver position, restricting charging freedom. In order to enable positional freedom for receivers, the new Tx coil proposed in this article provides omnidirectional magnetic field in a plane. This enables nearly constant coupling strength throughout all the receiver positions in 2-D omnidirectional space.

A. Proposed Cylindrical Transmitting Coil

The proposed cylindrical Tx coil is depicted in Fig. 2(a). The coil consists of two coaxial helical loops, which have wounded wires in the opposite directions. The two loops are placed in parallel in the *XY*-plane. The connection of two loops is arranged inside the coil in the shape of the letter Z. The main purpose of this arrangement is to minimize the unwanted magnetic field of the connecting wires, that would distort the uniformity of the charging field. Since the two loops maintain currents flowing in the opposite directions, the two loops effectively form a current loop whose field amplitude is uniform in the *XY* plane. The magnetic field magnitude and direction of the proposed coil are depicted in Fig. 2(b)–(d). It is clear that the magnetic field spreads isotropically in the *XY* plane.

Based on this key characteristic of the field distribution, Rx coils can be placed around the Tx coil at any position, offering full spacial freedom in the *XY* plane. Additionally, as the two helical loops are connected, the coil needs only one power supply without any active control.

It is evident that this twin Tx coil radiates weakly, as a *zz*-component of magnetic quadrupole tensor. Due to the coil symmetry, the magnetic dipole of the coil is fully suppressed. This means that the main channel of parasitic far-field radiation from the coil is totally blocked. In the available literature there are some works whose authors intentionally reduce the magnetic dipole moment of the Tx coil, while coupling to Rx devices is still provided by the field of this dipole moment. For example, in work [22] one suggested a planar spiral coil with the opposite direction of current in some turns. In work [23] one suggested an active control system switching planar loop turns with the opposite current direction depending on the distance between Tx and Rx. However, in both these cases the suppression of the
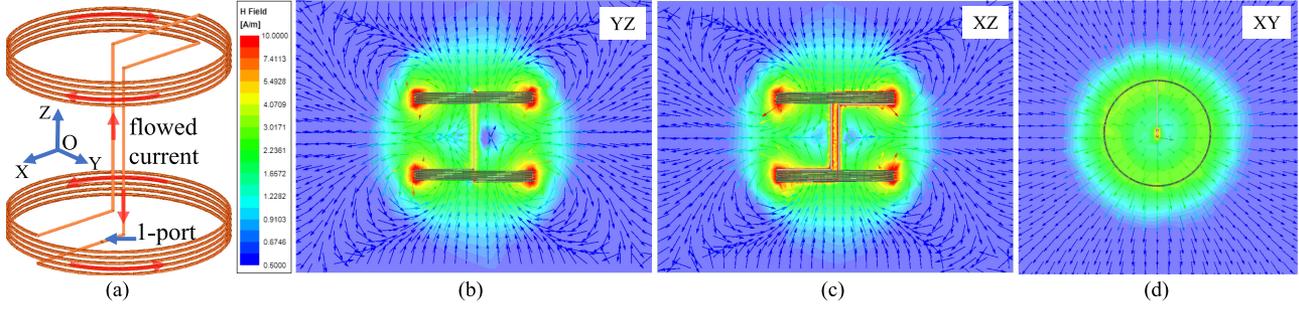
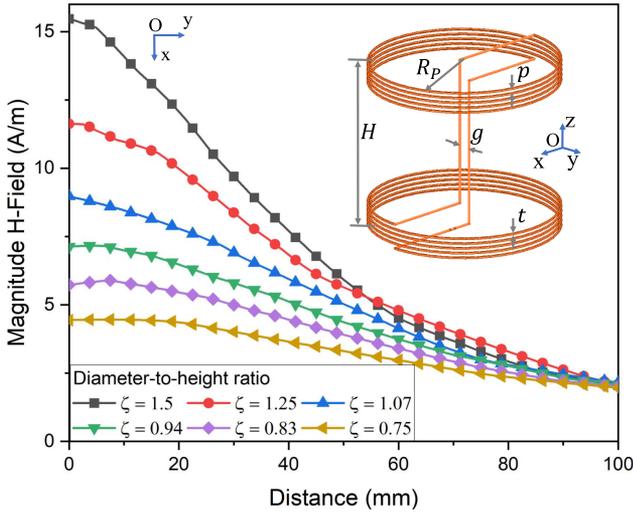Fig. 2. Proposed transmitting coil and its magnetic field magnitude and vectors in *YZ*, *XZ*, and *XY* planes.

Fig. 3. Magnetic field depending on the diameter-to-height ratios. The inset picture shows the cylindrical coil with its dimensions: $H = 140$, $R_P = 75$, $p = 5$, $g = 10$, $t = 2$, all units in mm. The diameter-to-height ratio is calculated by $\zeta = 2 \times R_P/H$.

Fig. 4. Geometry and the coordinate system.

magnetic dipole was only partial. Obviously, the aim of these works was very different: They aimed to improve misalignment tolerances for a directional WPT, and allowed active control, whereas we aim to obtain a 2-D ominidirectional WPT without any active control components. This allows us to completely suppress dipolar radiation.

In order to elaborate the effects of the coil diameter and height, we consider the dependence of the H-field with respect to changes of the diameter-to-height ratio of the coil, as shown in Fig. 3. When the diameter of the coil is larger than the height, the magnetic field decreases significantly with the increase of the transfer distance. In contrast, when the diameter is smaller than the height, the magnetic field is maintained better, but the field strength is weaker. Therefore, a compromise coil proportions have been chosen with moderate magnetic field strength and slow deterioration of the field at larger distances by selecting the diameter and the height of the coil being approximately equal. On the other hand, using higher numbers of turns, the coil can generate a stronger magnetic field. However, the intrinsic resistance and parasitic capacitance will also increase with an
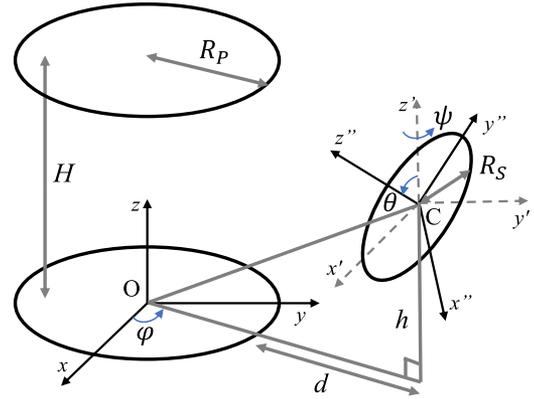
increase of the number of turns. We have analyzed the impact of parasitic resistance and capacitance, and found that in this case the only significant parasitic effects are due to ohmic resistance. However, its presence does not drastically change the optimal dimensions of the coil.

B. Mutual Inductance Verification

In order to estimate the performance of the proposed WPT transmitter, a mutual inductance assessment is necessary because of its rigid relation to the system performance. In this section, we investigate the mutual inductance between the proposed Tx coil and a planar spiral Rx coil. For the analytical calculations, the Tx is first modeled as a set of two coaxial circular current filaments of radius of R_P, distanced by H from each other, as shown in Fig. 4. The Rx coil is also modeled as a set of circular filaments with the radius R_S positioned at an inclined plane. The mutual inductance can be obtained for one turn of the first circular of the Tx coil and one turn of the Rx coil using the following expression [24]:

$$M_1|_i = \frac{\mu_0 R_S}{\pi} \int_0^{2\pi} \frac{[p_1 \cos\varphi + p_2 \sin\varphi + p_3]\Psi(k)}{k\sqrt{V_0^3}} d\varphi \quad (1)$$

where μ_0 is the permeability of free space, and the other parameters are explained in the Appendix. The total mutual inductance

TABLE I
MUTUAL INDUCTANCE COMPARISON AS A FUNCTION OF DISTANCE
(CALCULATION VERSION MEASUREMENT) $[\theta = 90°, \psi = 0°, h = 55$ MM]

M (nH)	0 cm	1 cm	2 cm	3 cm	4 cm	5 cm
Calc.	756	616	491.8	390.9	311.4	249.3
Meas.	750	590	465	342.5	275	212.5
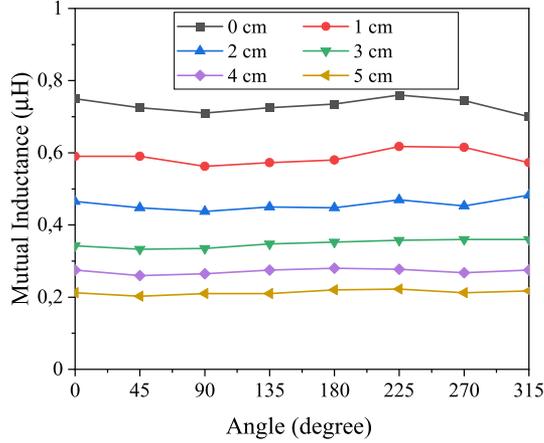
Fig. 5. Measured mutual inductance with $\theta = 90°$, $\psi = 0°$, and $h = 55$ mm.

between the Tx and Rx coils is given by

$$M = \sum_{k=1}^{N_S} M_k|_i = \sum_{k=1}^{N_S}\sum_{i=1}^{N_{P+}} M_k|_i - \sum_{k=1}^{N_S}\sum_{j=1}^{N_{P-}} M_k|_j \quad (2)$$

where N_{P+} and N_{P-} are the numbers of Tx turns in which the current flows in the same and opposite directions with the current in the Rx circular, respectively, and N_S is the number of Rx turns.

Table I shows a comparison of the mutual inductance between the calculated and measured results in the case of $h = 55$ mm, $\theta = 90°$, five turns for each Tx and Rx coils, for various distances. The mutual inductance was measured using the so-called antiparallel connection method [25]. There is a good agreement between the calculated and measured results. The mutual inductance between the Tx and Rx coils is measured at all angles at various distances, as shown in Fig. 5. Importantly, the mutual inductance is stable when the Rx rotates around the Tx coil at a certain distance. For short distances, the mutual inductance slightly fluctuated due to inaccuracies in the fabrication of the coil. At larger distances, the mutual inductance decreases as compared with closer placements, but it is almost constant for all angles.

C. Circuit Model and System Analysis

The schematic of the WPT system is shown in Fig. 6(a). In this system, a push–pull class-EF$_2$ inverter is used to supply power to the Tx coil, while a full-bridge rectifier is utilized to convert the received power to dc. The Tx and Rx coils are augmented by compensating capacitors C_2 and C_4, respectively. The system is designed to operate at 6.78 MHz. At this *high* frequency,
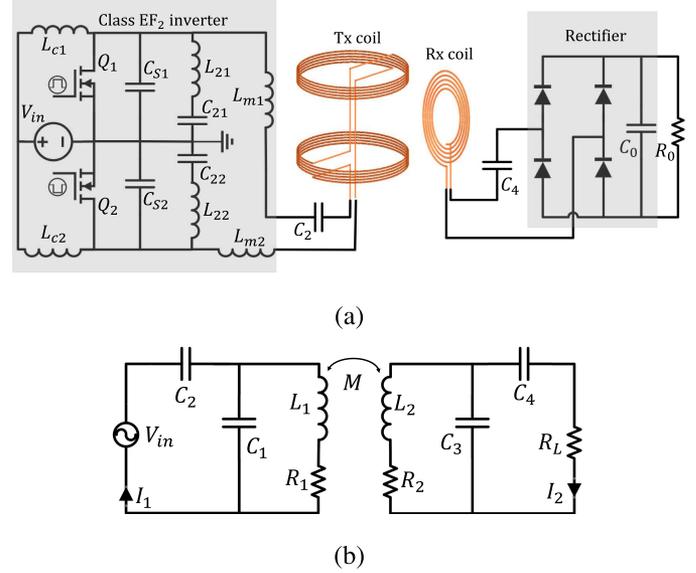
Fig. 6. (a) Schematic of the WPT system and (b) equivalent circuit.

parasitic capacitance of the coil of this complex structure is significant and cannot be neglected. Therefore, the topology of the equivalent circuit should take into account this capacitance, as shown in Fig. 6(b). The equivalent circuit is then composed of two resonant circuits corresponding to the Tx and Rx coils, which are coupled via a mutual inductance M. Consequently, each coil is represented by two branches in parallel: An inductor is connected in series with a parasitic resistor, and another branch is a shunt parasitic capacitor. A source with an intrinsic resistance is connected at the Tx side, while the Rx side is connected to a load resistor.

To achieve the maximum wireless link efficiency, the compensation capacitor must correctly resonate with the coil inductance. In other words, the reactance of the coil must be canceled by the compensation capacitance at the operating angular frequency $\omega = 2\pi \cdot 6.78 \cdot 10^6$ rad/s, corresponding to

$$C_2 = \frac{2C_1 L_1 \omega^2 - 1 - C_1^2 \omega^2 (R_1^2 + L_1^2 \omega^2)}{-L_1 \omega^2 + C_1^2 \omega^2 (R_1^2 + L_1^2 \omega^2)}$$
$$C_4 = \frac{2C_3 L_2 \omega^2 - 1 - C_3^2 \omega^2 (R_2^2 + L_2^2 \omega^2)}{-L_2 \omega^2 + C_3^2 \omega^2 (R_2^2 + L_2^2 \omega^2)}. \quad (3)$$

The WPT efficiency, η_{WPT}, is calculated as

$$\eta_{\text{WPT}} = \frac{I_2^2 R_L}{I_1^2 Z_1 + I_2^2 (Z_2 + R_L)}$$
$$= \frac{R_L \omega^2 M^2}{Z_1 (Z_2 + R_L)^2 + \omega^2 M^2 (Z_2 + R_L)} \quad (4)$$

and the corresponding optimal load $R_{L,\text{opt}}$ is

$$R_{L,\text{opt}} = Z_2 \sqrt{1 + \frac{\omega^2 M^2}{Z_1 Z_2}} \quad (5)$$

TABLE II
LUMPED ELEMENT VALUES OF THE RESONANT LOOPS

Tx		Rx	
Parameter	Value	Parameter	Value
L_1	11.9 μH	L_2	3 μH
C_1	12.4 pF	C_3	8.4 pF
C_2	33.9 pF	C_4	175.2 pF
R_1	2.85 Ω	R_2	0.36 Ω
Q_1	178.6	Q_2	366.7

Fig. 7. Experimental configuration for measurements.

where Z_1 and Z_2 are the equivalent impedances of the Tx and Rx coil, respectively, which are given by

$$Z_1 = \frac{R_1}{C_1^2 R_1^2 \omega^2 + (C_1 L_1 \omega^2 - 1)^2}$$
$$Z_2 = \frac{R_2}{C_3^2 R_2^2 \omega^2 + (C_3 L_2 \omega^2 - 1)^2}. \tag{6}$$

The parameters of the actual Tx and Rx coils are measured, and the results are shown in Table II. The parasitic capacitance C_1 of the Tx coil is much higher than C_3 of the Rx coil due to the complexity of the Tx structure. Similarly, the parasitic resistance R_1 of the Tx coil is also larger than R_2 of the Rx coil because of the long copper wire used to fabricate the coil. However, both of them are not too high thanks to the 2-mm diameter solid copper wire employed in this work. Therefore, the quality factors of both coils are sufficiently high, which helps to optimistically predict the efficiency of the system based on figure-of-merit $k\sqrt{Q_1 Q_2}$ [26]. To obtain high quality factors, the skin and proximity losses are reduced by winding the coil turns with the pitch approximately 2.5 times of the copper wire diameter for both Tx and Rx coils [27].

III. EXPERIMENTAL VERIFICATION OF THE WPT SYSTEM

A. Experimental Setup

The experimental setup of the WPT system is shown in Fig. 7. It consists of a commercial push–pull class EF_2 inverter GSWP300W-EVBPA, a dc power supply RIGOL DP832 A, two resonant coils, a full-bridge rectifier based on Schottky FSV10120 V diodes, and a resistive load. An oscilloscope is used to display the current and voltage at the Tx coil. In this work, the experimental dc–dc efficiency $\eta_{\text{DC–DC}}$ is calculated
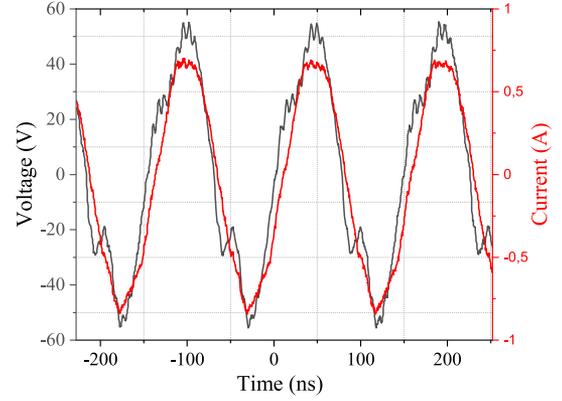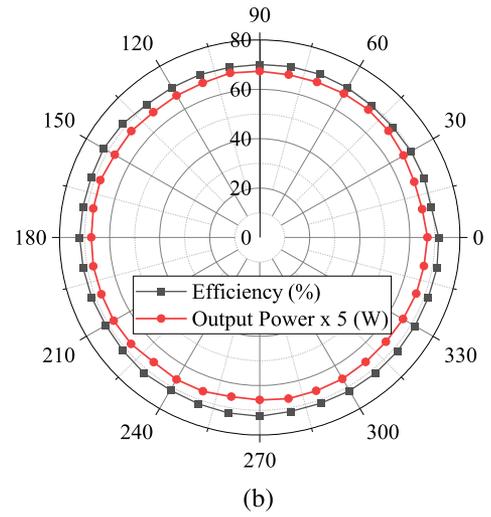
Fig. 8. (a) Voltage and current waveform at the Tx coil. (b) DC–DC efficiency and output power depending on the polar angle of the Rx coil.

as the ratio of the dc output power to the dc input power

$$\eta_{\text{DC–DC}} = \frac{P_{\text{out}}}{P_{\text{in}}} = \eta_{\text{inv}} \cdot \eta_{\text{WPT}} \cdot \eta_{\text{rec}} \tag{7}$$

where η_{inv}, η_{WPT}, and η_{rec} are the efficiencies of the inverter, WPT link, and rectifier, respectively. By using the dc–dc efficiency, all losses of each module, i.e., class EF_2 inverter, the WPT link between the Tx cylinder and planar Rx, and the full-bridge rectifier are included in the evaluation of the WPT system performance.

For the calculations of input and output power, FLUKE 28Π true-rms meters are used to measure the current and voltage at the input and the load.

B. Experimental Results

Fig. 8(a) shows the waveforms of the current and voltage at the Tx resonator. They are nearly in phase due to the good turning of the compensate capacitors at the operating frequency to cancel out the imaginary part of the coil impedance. The output power and dc–dc efficiency of the WPT system are demonstrated in Fig. 8(b) when the Rx coil is moved in the horizontal plane
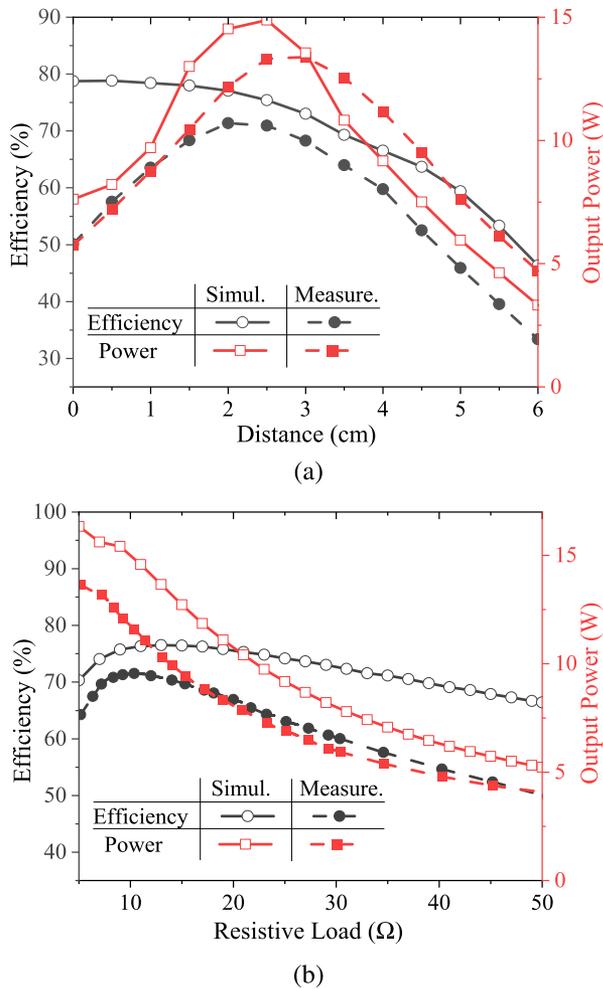
Fig. 9. DC–DC efficiency and output power depending on (a) distance d and (b) resistive load.

around the Tx coil keeping the distance $d = 2.5$ cm. It is obvious that the system efficiency can be maintained at approximately 70%. The minimum dc–dc efficiency is 69.6% at the polar angle of $10°$, while the maximum value is 72.4% at $270°$. Similarly, the output power also stays almost unchanged versus the rotation of the receiver position. The small deviation in the efficiency and power versus the polar angle of Rx is most probably caused by small defects of the fabrication and connection wires inside the Tx coil. Based on these experimental results, the proposed Tx coil is proved suitable for 2-D omnidirectional WPT. It has no *weak* or, moreover, *blind* angular regions in terms of efficiency and output power. In order to explore some additional features of the coil, we executed measurements for varying transfer distance, lateral and axial misalignments, and load resistance. An experiment for the dc–dc efficiency and output power validation was implemented to verify their dependence on the transfer distance and the load. The results are shown in Fig. 9. In this measurement, the Rx coil was placed at the angles $\theta = 90°$ and $\psi = 0°$. It was moved so that the distance d varied from 0 to 6 cm. One can see in Fig. 9(a) that the system efficiency stays above 50% when $d < 4.5$ cm. The output power reaches a peak of

13.38 W at the critical distance corresponding to the critical coupling coefficient [28]. At longer and shorter distances, the output power decreases due to the under and overcoupling phenomena, respectively. Overcoupling for short distances leads to detuning that results in a drop of the output voltage. Then the total conducting loss in the diodes of the rectifier becomes significant and comparable to the output power. This is why the efficiency of the system decreases, whereas for long distances it decreases due to insufficient mutual coupling. There is room for improvements of efficiency and transfer distance, which are possible with proper optimization in designs of application-specific realizations by using state-of-the-art engineering approaches. The WPT link efficiency can be enhanced by improving the coil quality factor with proper skin- and proximity-effect optimization to compensate for the low coupling coefficient [29]–[32]. In addition, using recent work on designs of very high-efficiency converters working at 6.78 MHz [33] one can achieve significantly better converter efficiency than in our laboratory test. In our work, the experimental results verify the main contributions of the new coil for truly 2-D omnidirectional WPT with a reasonable level of efficiency.

To investigate the dependence of the efficiency and output power on the load resistance, we made a measurement with the Rx coil at a fixed distance $d = 2.5$ cm. As it is seen in Fig. 9(b), the efficiency reaches the highest value with the optimal load of $10.37\ \Omega$. However, the matching is quite robust: When the load varies from $5\ \Omega$ to $50\ \Omega$, the efficiency keeps higher than 50%. It decreases significantly only beyond this interval of the load resistances. The output power also degrades similarly. The load dependence of the proposed WPT system is the same as that of conventional WPT systems based on usual coils. Optimization of the load dependence has been investigated in [34]–[36]. The results of these works may be used for optimizing the load response of the proposed WPT system, as well.

We have studied the impact of lateral and axial misalignments. To validate the robustness to axial misalignments, the Rx coil was initially placed at a distance of 3 cm, and then rotated around its vertical diameter so that the rotation angle ψ shown in the inset of Fig. 10(a) varied from $-40°$ to $40°$. The efficiency as well as the output power decrease with this rotation quite weakly. When $\psi = \pm 40°$ the efficiency drops only by 5%, and the output power decreases from 12.8 to 11.3 W. This is so because the area of the Rx coil is sufficient to respond not only to the radial component of the magnetic field created by the Tx coil but also to the angular component. Though in the symmetry plane $z = H/2$ at the distance $d = \sqrt{x^2 + y^2} = 3$ cm the magnetic field is purely radial, around this point the azimuthal component has the same order of magnitude. Thus, the Rx coil can be noticeably rotated around the vertical axis without significant deterioration of power transfer.

Further, starting from the same distance $d = 3$ cm, the Rx coil was moved in the horizontal and vertical directions to verify the performance of the system versus lateral displacements. As one can see in Fig. 10(b), both efficiency and output power reduce only by 9% when the Rx is shifted up to 5 cm from the optimal position along the horizontal axis parallel to the loop plane. However, the decline is significant versus the vertical
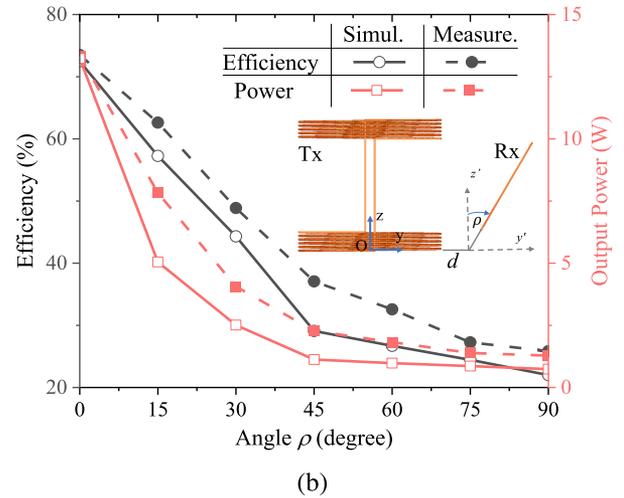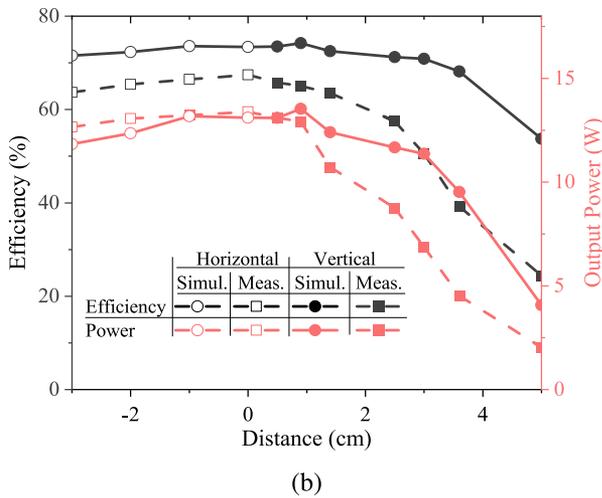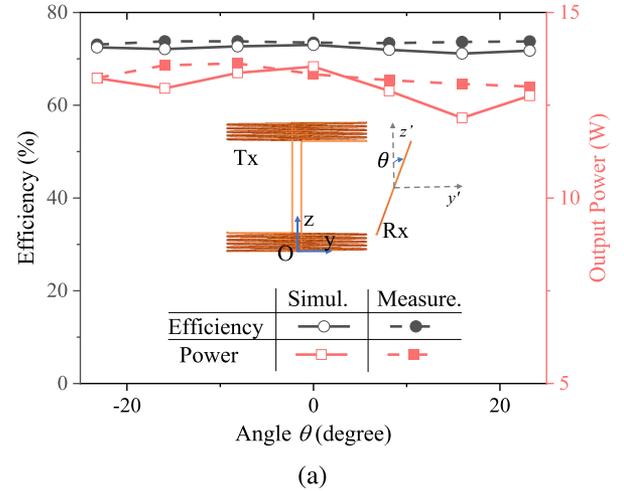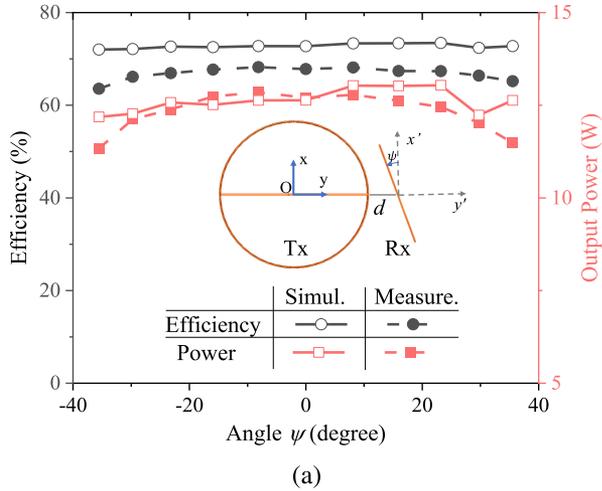
Fig. 10. DC–DC efficiency and output power depending on (a) Rx rotation angle, (b) horizontal, and vertical displacements of the Rx coil.

Fig. 11. Our system dc–dc efficiency and output power depending on (a) the θ angle and (b) the ρ angles. Both angles are shown on the insets.

displacement. When we shift the loop up or down by the same 5 cm, the efficiency drops from 67% to 25%, and the output power decays from 13.4 to 2 W. Indeed, the magnetic field generated by the Tx coil has the uniform and homogeneous magnitude only in the horizontal plane, not in the vertical planes. To charge a single device at a specific position, a vertical or tilted holder is useful [40]. In our design, a groove or a stand ring can be used to hold many Rx devices placed around with a diversity of possible orientations.

Finally, we have studied robustness to tilts of the Rx coil. In the first scenario the Rx coil is tilted so that its center remains at the same distance $d + R_p$ from the axis of the Tx coil [θ angle in Fig. 11(a)]. When the Rx coil rotates this way, while the upper half of the loop moves away from Tx, the lower half of the Rx coil comes closer to the Tx coil. In the 2-D scenario, the distance $d = 3$ cm is fixed between the edges of the Rx and Tx coils, as it is shown in the inset of Fig. 11(b). In the first scenario the efficiency and power are not sensitive to tilts up to $\theta = 20°$ when the Rx coil responds well to the magnetic field which is basically horizontal. In the second scenario, the efficiency and power worsen with increasing ρ angle because

this tilt is accompanied by an increase of the distance between the centers of the Tx and Rx coils. Nevertheless, the efficiency of the WPT system keeps above 50% until θ and ρ attain 30°.

IV. SAR VERIFICATION AND PERFORMANCE COMPARISON

Based on the above investigations of the proposed 2-D omnidirectional WPT system, it is clear that the proposed Tx coil is a superior candidate consumer applications, such as portable and mobile wireless charging, in terms of the performance and the omnidirectionality. A hypothetical context of the wireless charging for mobile use of the proposed Tx structure is demonstrated in Fig. 12(a). Here, we evaluate the exposure safety of the human body for such WPT system. In this application scenario, the human hand holding the mobile device is the closest body part to the charging module. Here, in this SAR simulation, we assume that the user may bring the hand close to the device if he/she wants to operate the phone during the charging process. This hand position also corresponds to the time when the user brings the device to the holder (or takes it back). The electromagnetic field absorption is certified by the SAR value, which determines

TABLE III
COMPARISON OF STATE-OF-THE-ART 2-D OMNIDIRECTIONAL WPT SYSTEMS

| Ref.	Coil structure	Source	Control method	Frequency	Dimension Tx/Rx	Distance center-center	Efficiency	Output power
[18].2017	Orthogonal	multiple	nonidentical current	535 kHz	30/30 cm	30 cm	∼ 78 %	∼ 0.5 W
[19].2015	Orthogonal	multiple	load detection and power flow	550 kHz	30/30 cm	30 cm	69.5 %	1 W
[20].2018	Cubic Tx	single	none	13.56 MHz	20/20 cm	30 cm	max 60 % (non-uniform)	10 W
[37].2019	Orthogonal	multiple	independent control of sources	20 kHz	30/10 cm	21 cm	11.5 %	9.42 W
[38].2020	Cylinder	multiple	three-phase inverter	85 kHz	–	–	–	5.57 W
[39].2012	Separate orthogonal	single	none (only multidirectional)	15.1 MHz	30/30 cm	20 cm	0°: 40.07 % 45°: 74.08 %	–
This work	Cylindrical	single	none	6.78 MHz	15/10 cm	10 cm	72 % DC-DC	13.5 W
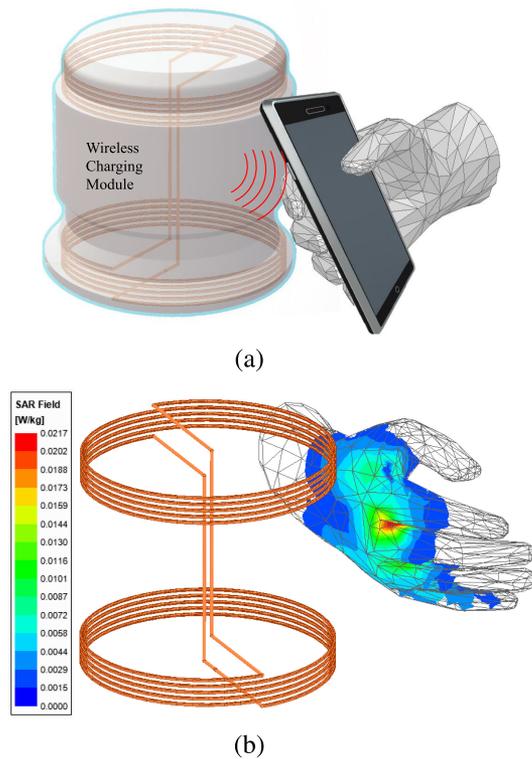
Fig. 12. (a) Hypothetical context of a consumer application and (b) SAR simulation setup and results.

the absorbed power in the human body. Depending on the human body parts, there are different limitations in the SAR regulations. For example, under the IEEE safety regulation [41], the maximum SAR value for whole-body exposure is 0.08 W/kg, for head and trunk is 2 W/kg, and for limbs and pinnae it is 4 W/kg. In this article, the SAR is numerically simulated in ANSYS high-frequency structure simulator (HFSS) tool. A human hand model was used to verify the exposure at a distance of 2.5 cm in this application scenario. Fig. 12(b) shows the simulation setup and calculated SAR values. The SAR value is approximately 21.7 mW/kg averaging over 1 g of tissue, which is much smaller than the limitation for limbs in the safety regulations. With the low SAR rate, the proposed Tx coil allows one to increase the power level significantly, still keeping it safe in consumer applications. Finally, a comparative analysis between the proposed

WPT system and known alternative structures is presented in Table III. Known structures are based on orthogonal coils with complex control methods, which require multiple sources and are costly [18], [19], [37], [38]. In order to simplify control circuits, some structures using different transmitter topology were proposed, however, the 2-D omnidirectional characteristic was not obtained properly in all receiving angles [20], [21], [39]. On the other hand, the cylindrical Tx coil proposed in this article offers a completely 2-D omnidirectional WPT system with a single source.

V. CONCLUSION

In this article, we have proposed and studied a new cylindrical Tx coil for 2-D omnidirectional WPT systems, especially for mobile and portable wireless charging applications. The magnetic field of the Tx coil shape inherently exhibits the desired omnidirectional characteristic without any active control or tuning. In addition, the mutual inductance between the proposed Tx coil and a spiral Rx coil was studied. With the complexity of the coil, the parasitic capacitance of the coil was considered and modeled in the equivalent circuit, and then mathematically analyzed for various generic cases. From the experimental results, it was seen that the proposed Tx coil can transfer power to the Rx coil placed around it with a dc-to-dc efficiency of up to 72.4% at a power level of 13 W and operating frequency of 6.78 MHz. The system efficiency and output power dependence on the transfer distance, vertical/horizontal movements, and rotating angles were studied to validate the performance of the system. Finally, a hypothetical scenario of consumer application on mobile charging was demonstrated with a SAR assessment based on the human safety regulations. In conclusion, the use of the proposed cylindrical Tx coils gives advantages of low-cost fabrication and omnidirectional charging possibility in practical consumer applications. The multireceiver use of the proposed WPT coil would be the following research direction leading to real-life applications.

The same functionality can be achieved with two separate sources feeding the top and bottom coils. However, in order to drive the strictly opposite currents in the coils, both power sources need to be synchronized (for example, using two inverters driven by the same pulse generator). This approach may offer a possibility to increase the transferred power level.

Finally, we note that the proposed coil structure has an important advantage of extremely weak parasitic radiation of power into surrounding space. The current distribution is equivalent to two closely positioned collinear magnetic dipoles of the opposite orientation. Thus, the dominant dipole-mode radiation is effectively compensated. This feature makes the proposed coil most suitable for high-frequency WPT systems.

APPENDIX

The Rx circular is located in the inclined plane, in general defined by

$$ax + by + cz + d = 0. \tag{8}$$

The parameters a, b, and c defining the center of the Rx coil can be expressed as

$$\begin{aligned} a &= \sin\psi\sin\theta \\ b &= -\cos\psi\sin\theta \\ c &= \cos\theta. \end{aligned} \tag{9}$$

The parameters in (1) are given by [24]

$$\alpha = \frac{R_S}{R_P}, \ \beta = \frac{x_C}{R_P}, \ \gamma = \frac{y_C}{R_P}, \ \delta = \frac{z_C}{R_P}$$

$$l = \sqrt{a^2 + b^2}, \ L = \sqrt{a^2 + b^2 + c^2}$$

$$p_1 = \pm\frac{\gamma c}{l}, \ p_2 = \mp\frac{\beta l^2 + \gamma ab}{lL}, \ p_3 = \frac{\alpha c}{L}$$

$$A_0 = 1 + \alpha^2 + \beta^2 + \gamma^2 + \delta^2 + 2\alpha(p_4\cos\varphi + p_5\sin\varphi)$$

$$V_0^2 = \alpha^2\left[\left(1 - \frac{b^2c^2}{l^2L^2}\right)\cos^2\varphi + \frac{c^2}{l^2}\sin^2\varphi + \frac{abc}{l^2L}\sin2\varphi\right]$$
$$+ \beta^2 + \gamma^2 \mp 2\alpha\frac{\beta ab - \gamma l^2}{lL}\cos\varphi \pm \frac{2\alpha\beta c}{l}\sin\varphi,$$

$$k = \sqrt{\frac{4V_0}{A_0 + 2V_0}}, \ \Psi(k) = \left(1 - \frac{k^2}{2}\right)K(k) - E(k) \tag{10}$$

where $(x_C, y_C, \text{ and } z_C)$ is the center of the Rx coil, and $K(k)$ and $E(k)$ denote the complete elliptic integrals of the first and second kind [24].

REFERENCES

[1] A. Kurs, A. Karalis, R. Moffatt, J. D. Joannopoulos, P. Fisher, and M. Soljacic, "Wireless power transfer via strongly coupled magnetic resonances," *Science*, vol. 317, no. 5834, pp. 83–86, 2007.

[2] H. Hoang, S. Lee, Y. Kim, Y. Choi, and F. Bien, "An adaptive technique to improve wireless power transfer for consumer electronics," *IEEE Trans. Consum. Electron.*, vol. 58, no. 2, pp. 327–332, May 2012.

[3] C. J. Chen, T. H. Chu, C. L. Lin, and Z. C. Jou, "A study of loosely coupled coils for wireless power transfer," *IEEE Trans. Circuits Syst. II: Exp. Briefs*, vol. 57, no. 7, pp. 536–540, Jul. 2010.

[4] N. Ha-Van and C. Seo, "Modeling and experimental validation of a butterfly-shaped wireless power transfer in biomedical implants," *IEEE Access*, vol. 7, pp. 107225–107233, 2019.

[5] Z. N. Low, R. A. Chinga, R. Tseng, and J. Lin, "Design and test of a high-power high-efficiency loosely coupled planar wireless power transfer system," *IEEE Trans. Ind. Electron.*, vol. 56, no. 5, pp. 1801–1812, May 2009.

[6] N. Nguyen, N. Ha-Van, and C. Seo, "Midfield wireless power transfer for deep-tissue biomedical implants," *IEEE Antennas Wireless Propag. Lett.*, vol. 19, no. 12, pp. 2270–2274, Dec. 2020.

[7] P. K. S. Jayathurathnage, X. Dang, C. Simovski, and S. Tretyakov, "Self-tuning omnidirectional wireless power transfer using double toroidal helix coils," *IEEE Trans. Ind. Electron.*, vol. 69, no. 7, pp. 6828–6837, Jul. 2022.

[8] J. Li, Y. Yang, H. Yan, C. Liu, L. Dong, and G. Wang, "Quasi-omnidirectional wireless power transfer for a sensor system," *IEEE Sensors J.*, vol. 20, no. 11, pp. 6148–6159, Jun. 2020.

[9] Z. Zhang and B. Zhang, "Angular-misalignment insensitive omnidirectional wireless power transfer," *IEEE Trans. Ind. Electron.*, vol. 67, no. 4, pp. 2755–2764, Apr. 2020.

[10] J. Feng, Q. Li, F. Lee, and M. Fu, "Transmitter coils design for free-positioning omnidirectional wireless power transfer system," *IEEE Trans. Ind. Informat.*, vol. 15, no. 8, pp. 4656–4664, Aug. 2019.

[11] J. Wang et al., "Lateral and angular misalignments analysis of a new PCB circular spiral resonant wireless charger," *IEEE Trans. Magn.*, vol. 48, no. 11, pp. 4522–4525, Nov. 2012.

[12] J. Kim, D.-H. Kim, and Y.-J. Park, "Free-positioning wireless power transfer to multiple devices using a planar transmitting coil and switchable impedance matching networks," *IEEE Trans. Microw. Theory Techn.*, vol. 64, no. 11, pp. 3714–3722, Nov. 2016.

[13] K. Na, H. Jang, H. Ma, and F. Bien, "Tracking optimal efficiency of magnetic resonance wireless power transfer system for biomedical capsule endoscopy," *IEEE Trans. Microw. Theory Techn.*, vol. 63, no. 1, pp. 295–304, Jan. 2015.

[14] O. Jonah, S. V. Georgakopoulos, and M. M. Tentzeris, "Orientation insensitive power transfer by magnetic resonance for mobile devices," in *Proc. IEEE Wireless Power Transfer*, 2013, pp. 5–8.

[15] W. M. Ng, C. Zhang, D. Lin, and S. R. Hui, "Two-and three-dimensional omnidirectional wireless power transfer," *IEEE Trans. Power Electron.*, vol. 29, no. 9, pp. 4470–4474, Sep. 2014.

[16] J. Feng, Q. Li, and F. Lee, "Load detection and power flow control algorithm for an omnidirectional wireless power transfer system," *IEEE Trans. Ind. Electron.*, vol. 69, no. 2, pp. 1422–1431, Feb. 2022.

[17] B. H. Choi, E. S. Lee, Y. H. Sohn, G. C. Jang, and C. T. Rim, "Six degrees of freedom mobile inductive power transfer by crossed dipole Tx and Rx coils," *IEEE Trans. Power Electron.*, vol. 31, no. 4, pp. 3252–3272, Apr. 2016.

[18] D. Lin, C. Zhang, and S. Y. R. Hui, "Mathematical analysis of omnidirectional wireless power transfer-Part-I: Two-dimensional systems," *IEEE Trans. Power Electron.*, vol. 32, no. 1, pp. 625–633, Jan. 2017.

[19] C. Zhang, D. Lin, and S. Hui, "Basic control principles of omnidirectional wireless power transfer," *IEEE Trans. Power Electron.*, vol. 31, no. 7, pp. 5215–5227, Jul. 2016.

[20] N. Ha-Van and C. Seo, "Analytical and experimental investigations of omnidirectional wireless power transfer using a cubic transmitter," *IEEE Trans. Ind. Electron.*, vol. 65, no. 2, pp. 1358–1366, Feb. 2018.

[21] C. Lu et al., "Design and analysis of an omnidirectional dual-band wireless power transfer system," *IEEE Trans. Antennas Propag.*, vol. 69, no. 6, pp. 3493–3502, Jun. 2021.

[22] J. Kim and J. Jeong, "Range-adaptive wireless power transfer using multiloop and tunable matching techniques," *IEEE Trans. Ind. Electron.*, vol. 62, no. 10, pp. 6233–6241, Oct. 2015.

[23] Y. Zhuang, A. Chen, C. Xu, Y. Huang, H. Zhao, and J. Zhou, "Range-adaptive wireless power transfer based on differential coupling using multiple bidirectional coils," *IEEE Trans. Ind. Electron.*, vol. 67, no. 9, pp. 7519–7528, Sep. 2020.

[24] S. Babic, F. Sirois, C. Akyel, and C. Girardi, "Mutual inductance calculation between circular filaments arbitrarily positioned in space: Alternative to grover's formula," *IEEE Trans. Magn.*, vol. 46, no. 9, pp. 3591–3600, Sep. 2010.

[25] Y. P. Su, L. Xun, and S. Y. R. Hui, "Mutual inductance calculation of movable planar coils on parallel surfaces," *IEEE Trans. Power Electron.*, vol. 24, no. 4, pp. 1115–1123, Apr. 2009.

[26] S. Y. R. Hui, W. Zhong, and C. K. Lee, "A critical review of recent progress in mid-range wireless power," *IEEE Trans. Power Electron.*, vol. 29, no. 9, pp. 4500–4511, Sep. 2014.

[27] J. P. K. Sampath, A. Alphones, D. M. Vilathgamuwa, A. Ong, and X. B. Nguyen, "Coil enhancements for high efficiency wireless power transfer applications," in *Proc. IECON 40th Annu. Conf. IEEE Ind. Electron. Soc.*, 2014, pp. 2978–2983.

[28] A. P. Sample, D. T. Meyer, and J. R. Smith, "Analysis, experimental results, and range adaptation of magnetically coupled resonators for wireless power transfer," *IEEE Trans. Ind. Electron.*, vol. 58, no. 2, pp. 544–554, Feb. 2011.

[29] D.-H. Kim, J. Kim, and Y.-J. Park, "Optimization and design of small circular coils in a magnetically coupled wireless power transfer system in the megahertz frequency," *IEEE Trans. Microw. Theory Techn.*, vol. 64, no. 8, pp. 2652–2663, Aug. 2016.

[30] G. Zulauf and J. M. Rivas-Davila, "Single-turn air-core coils for high-frequency inductive wireless power transfer," *IEEE Trans. Power Electron.*, vol. 35, no. 3, pp. 2917–2932, Mar. 2020.

[31] T.-H. Kim, G.-H. Yun, W. Y. Lee, and J.-G. Yook, "Asymmetric coil structures for highly efficient wireless power transfer systems," *IEEE Trans. Microw. Theory Techn.*, vol. 66, no. 7, pp. 3443–3451, Jul. 2018.

[32] J. Lawson, D. C. Yates, and P. D. Mitcheson, "High Q coil measurement for inductive power transfer," *IEEE Trans. Microw. Theory Techn.*, vol. 67, no. 5, pp. 1962–1973, May 2019.

[33] L. Gu, G. Zulauf, Z. Zhang, S. Chakraborty, and J. Rivas-Davila, "Push-pull class ϕ_2 RF power amplifier," *IEEE Trans. Power Electron.*, vol. 35, no. 10, pp. 10515–10531, Oct. 2020.

[34] L. Roslaniec, A. S. Jurkov, A. A. Bastami, and D. J. Perreault, "Design of single-switch inverters for variable resistance/load modulation operation," *IEEE Trans. Power Electron.*, vol. 30, no. 6, pp. 3200–3214, Jun. 2015.

[35] W. D. Braun and D. J. Perreault, "A high-frequency inverter for variable-load operation," *IEEE Trans. Emerg. Sel. Topics Power Electron.*, vol. 7, no. 2, pp. 706–721, Jun. 2019.

[36] Q. Zhao, A. Wang, J. Liu, and X. Wang, "The load estimation and power tracking integrated control strategy for dual-sides controlled LCC compensated wireless charging system," *IEEE Access*, vol. 7, pp. 75749–75761, 2019.

[37] H. Han, H. Mao, Q. Zhu, M. Su, and A. P. Hu, "A 3D wireless charging cylinder with stable rotating magnetic field for multi-load application," *IEEE Access*, vol. 7, pp. 35981–35997, 2019.

[38] L. Tan *et al.*, "Power stability optimization design of three-dimensional wireless power transmission system in multi-load application scenarios," *IEEE Access*, vol. 8, pp. 91843–91854, 2020.

[39] D. Wang, Y. Zhu, H. Guo, X. Zhu, T. Mo, and Q. Huang, "Enabling multi-angle wireless power transmission via magnetic resonant coupling," in *Proc. 7th Int. Conf. Comput. Convergence Technol.*, 2012, pp. 1395–1400.

[40] C. Xu, Y. Zhuang, C. Song, Y. Huang, and J. Zhou, "Dynamic wireless power transfer system with an extensible charging area suitable for moving objects," *IEEE Trans. Microw. Theory Techn.*, vol. 69, no. 3, pp. 1896–1905, Mar. 2021.

[41] *IEEE Standard for Safety Levels With Respect to Human Exposure to Electric, Magnetic, and Electromagnetic Fields, 0 hz to 300 GHz*, IEEE Std. C95.1-2019 (Revision of IEEE Std. C95.1-2005/ Incorporates IEEE Std. C95.1-2019/Cor 1-2019), 2019.

Yining Liu received the B.Sc. and M.Sc. degrees in electrical engineering from Harbin Institute of Technology, Harbin, China, in 2018 and 2020, respectively. She is currently working toward the D.Sc. degree in electrical engineering with Aalto University, Espoo, Finland.

Her research interests include wireless power transfer, high-frequency dc–dc converters and MOSFET gate drivers.

Prasad Jayathurathnage (Member, IEEE) received the B.Sc. degree in electronics and telecommunications engineering from the University of Moratuwa, Moratuwa, Sri Lanka, in 2009, and the Ph.D. degree in electrical and electronic engineering from Nanyang Technological University, Singapore, in 2017.

He has been working with the Queensland University of Technology, Brisbane City, QLD, Australia and Rolls-Royce-NTU Corporate Lab, Singapore. He is currently a Postdoctoral Researcher with the School of Electrical Engineering, Aalto University, Espoo, Finland. His research interests include high-frequency power converters, wide-band-gap devices, and wireless power transfer.
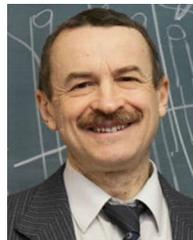
Constantin R. Simovski received the Ph.D. and doctor's of sciences (HDR) degrees in physics and mathematics from St. Petersburg State Polytechnic University, Saint Petersburg, Russia, in 1986 and 2000, respectively.

He was with both industry and academic institutions in several countries. From 2001 to 2008, he was a Full Professor with ITMO University, Saint Petersburg, Russia. Since 2008, he has been with Aalto University, Espoo, Finland, where he has been a Full Professor, since 2012. He had authored and coauthored three scientific monographs and over 230 papers in refereed journals. His research interests include metamaterials for optical sensing and energy harvesting, thermal radiation and radiative heat transfer on nanoscale, antennas for magnetic resonance imaging, and wireless power transfer.

Nam Ha-Van (Member, IEEE) received the B.S. degree in electronics and telecommunications engineering from the School of Electronics and Telecommunications, Hanoi University of Science and Technology, Hanoi, Vietnam, in 2012, and the Ph.D. degree in information and telecommunication engineering from Soongsil University, Seoul, South Korea, in February 2019.

He was a Postdoctoral Researcher with Soongsil University, from March 2019 to September 2020. He is currently a Postdoctoral Researcher with the Department of Electronics and Nanoengineering, School of Electrical Engineering, Aalto University, Espoo, Finland. His research interests include wireless power transfer, metamaterials, antennas, and energy harvesting systems.

Sergei A. Tretyakov (Fellow, IEEE) received the Dipl. Engineer-Physicist, candidate of sciences (Ph.D.), and D.Sc. degrees in radiophysics from Saint Petersburg State Technical University, Saint Petersburg, Russia, in 1980, 1987, and 1995, respectively.

From 1980 to 2000, he was with the Department of Radiophysics, Saint Petersburg State Technical University. He is currently a Professor of Radio Science with the Department of Electronics and Nanoengineering, Aalto University, Espoo, Finland. He was the President of the Virtual Institute for Artificial Electromagnetic Materials and Metamaterials (Metamorphose VI), from 2007 to 2013. He has authored or coauthored six research monographs and over 300 journal articles. His research interests include electromagnetic field theory, complex media electromagnetics, metamaterials, and microwave engineering.

Dr. Tretyakov served as the Chairman of the Saint Petersburg IEEE Electron Devices/Microwave Theory and the Techniques/Antennas and Propagation Chapter, from 1995 to 1998, and the General Chair of the International Congress Series on Advanced Electromagnetic Materials in Microwaves and Optics (Metamaterials).